Investigation on Effect of Some Operating Conditions on Flow and Heat Transfer of Supercritical CO2 In Helical Coiled Tubes via Multilevel Factorial Methodology

D. Devandran[1,a], A. N. Oumer [2,b,*], N. T. Rao[1,c],
F. Basrawi[1,d], H. Ibrahim[1,e]

[1,2,3,4,5]Faculty of Mechanical Engineering, University of Malaysia Pahang, Pekan, Malaysia

[a]devandrangunasegar@gmail.com, [b]ahmnur99@gmai.com, [c]thiwaan@hotmail.com, [d]mfirdausb@ump.edu.my

*Corresponding author :
ahmnur99@gmail.com

Abstract

In order to optimize the thermal-hydraulic performance of supercritical carbon dioxide (scCO$_2$) flowing through helically coiled tubes, the main and interaction effects of two operating parameters such as inlet pressure, and inlet mass flow rate on the Nusselt number and friction factor was investigated by applying a multilevel factorial design (MFD) analysis. The developed model is intended to analyze the friction factor (f) and Nusselt number (Nu) of heating process using scCO$_2$ as a working fluid using two-factor and three-level MFD method. Three different inlet pressures (8.00 MPa, 9.03 MPa and 10.05 MPa) with three different inlet mass fluxes (0.0131 m^3/s, 0.0151 m^3/s and 0.0167 m^3/s) at constant inlet temperature of 27 °C are considered. It was observed from the simulation results that inlet pressure has no significant effect on the Nusselt number while varying the mass flow rate affected the Nu significantly. On the other hand, increments of both inlet pressure and mass flux have decreased the friction factor. The MFD studies showed that for the Nusselt number, mass flow rate was found to be the most significant factor followed by the pressure in terms of importance. However, in case of friction factor, inlet pressure was the most significant factor. In general, it is proved from this study that a multilevel-factorial design was an effective method for determining the influences of inlet pressure and mass flow rate on the thermal-hydraulic performance of scCO$_2$ heating process.

Keywords: scCO$_2$; factorial design method; optimization; heat transfer.

1.0 INTRODUCTION

Most of the energy stored in one place is transferred to another place in a form of heat energy either by natural or forced convection which depends on the conditions of flow. Some fluids such as carbon dioxide (CO$_2$) gas are used to enhance such heat transfer processes. CO$_2$ is an environmental friendly gas that has been reintroduced recently as it has zero ozone depleting (ODP) and zero effective global warming potential (GWP) [1]. Furthermore, it is non-toxic, abundant and non-combustible. CO$_2$ has unique heat transfer properties at its supercritical state. Hence, using

supercritical carbon dioxide (scCO2) can be ideal replacement for these non-environmental friendly refrigerants with the suitable thermophysical properties and appropriate model of heat exchanger design. scCO2 fluid is neither in liquid nor in gas state and this behavior occurs when the pressure and temperature reach to 7.39 MPa and 31.1°C, respectively [2]. At the point where scCO2 reaches near to critical point, the thermo-physical properties show extremely rapid variations with a change in temperature and pressure [3]. The thermo-physical properties of scCO2 such as density (ρ), specific heat capacity (C_p), viscosity (μ) and thermal conductivity (k) can be obtained from the chemistry web book of National Institute of Science and Technology (NIST) [4].

The type of heat exchanger used to study the characteristics of scCO2 by some researches are mostly in the form of vertical and/or horizontal tubes, miniatures, plates, fins and coils. Most of the heat exchangers are made up of stainless steel material [5]. Moreover, many studies have been conducted by researchers on scCO2 using one or two parameters for cooling or heating processes [6]. However, research shows that there is still an enormous interest in this field. Interesting studies are available, although they are limited in terms of factors variability. Heat transfer enhancement using scCO2 as working fluid is a complex process, and disregarding the interaction of factors may result in erroneous conclusions. A reliable solution to this problem would be to consider all interaction effects as well as main effects. For this reason, a design of experiments method, called multilevel factorial design (MFD) could be helpful to optimize the heat transfer process. MFD is a multi-factor cross-group design. It not only can test the differences between various levels of factors, but also can test the interaction between the factors. This method requires greater number of experiments compared with fractional design or Taguchi method and provides very accurate results on the interaction between any two factors [7].

The main purpose of the current study is to investigate the effect of operating parameters to optimize the thermal-hydraulic performance of scCO2 in coiled tubes via the MFD method. The important operating conditions such as inlet pressures (8–10 MPa), and inlet mass fluxes (0.013–0.0167 m³/s) were chosen so as to study their main and interaction effects on the responses: Nusselt number and friction. A regression model was presented for each response and optimization of the process was carried out to maximize the Nusselt number (heat transfer) and minimize friction factor (pressure drop). Finally, the thermal-hydraulic performance of scCO2 flowing through helically coiled tubes under optimum

conditions was investigated for using in industrial applications.

2.0 NUMERICAL DETAILS

Governing Equations

In this study, the flow field is assumed to be incompressible, steady and non-isothermal. Therefore, the governing equations for the continuity, momentum and energy can respectively be expressed as [6, 8-11]:

$$\vec{\nabla} \cdot \vec{V} = 0 \qquad (1)$$

$$\rho \frac{D\vec{V}}{Dt} = \rho \left[\frac{\partial \vec{V}}{\partial t} + (\vec{\nabla} \cdot \vec{V})\vec{V} \right] = -\vec{\nabla}P + \rho\vec{g} + \mu\vec{\nabla}^2\vec{V} \qquad (2)$$

$$\rho C_P \left(\frac{\partial T}{\partial t} + \vec{V} \cdot \vec{\nabla}T \right) = k\vec{\nabla}^2 T + \dot{\gamma} \cdot \tau \qquad (3)$$

where $\vec{\nabla}$ is divergence operator and V is thee velocity vector of the fluid (m/s), ρ is density of the fluid (kg/m³), t is time (seconds), P is the hydrostatic pressure (Pa), g is gravitational acceleration (m/s²) and μ in the fluid viscosity (kg/m.s). C_P is the specific heat (J/kg.K), and k is the thermal conductivity (W/m.K). The term $\dot{\gamma}$ represents the shear rate, and τ is the total stress tensor.

Data reduction

The friction in the tube causes pressure loss when a fluid flows through it. The friction factor can be calculated with the pressure drop (ΔP) equation [8]. The general equation of f is:

$$f = \frac{2D\Delta P}{\rho V^2 L} \qquad (4)$$

where ΔP is pressure drop (Pa), L is length of the tube (m), and D is diameter of the tube (m).

In addition to the friction factor, the convective heat transfer rate ($\dot{Q}_{conv}$) can also be calculated with the following Newton's Law of Cooling expression [12]:

$$\dot{Q}_{conv} = hA_S \left(T_S - T_\infty \right) \qquad (5)$$

where $\dot{Q}_{conv}$ is convection heat transfer rate (W), h is convection heat transfer coefficient (W/m2 °C), A_S is surface area (m²) , T_S is surface temperature (°C) and T_∞ is fluid temperature (°C). The Nusselt number (Nu) was calculated using the following equation:

$$Nu = \frac{hD}{k} \qquad (6)$$

Computational Domain and Boundary Conditions

In order to conduct numerical simulation for this project, a circular type of helical coil tube was designed in 3D model using SolidWorks software as shown in Fig. 1. The helical coil tube is considered and designed using single inlet and single outlet with all the dimensions in mm according to the experimental work of Xu. J. et.al. [13]. The material used for the helical coiled tube is stainless steel as this material is used by previous researchers in their experimental studies. Table 1 shows the dimensions used to design the numerical model of the helical coiled tube.
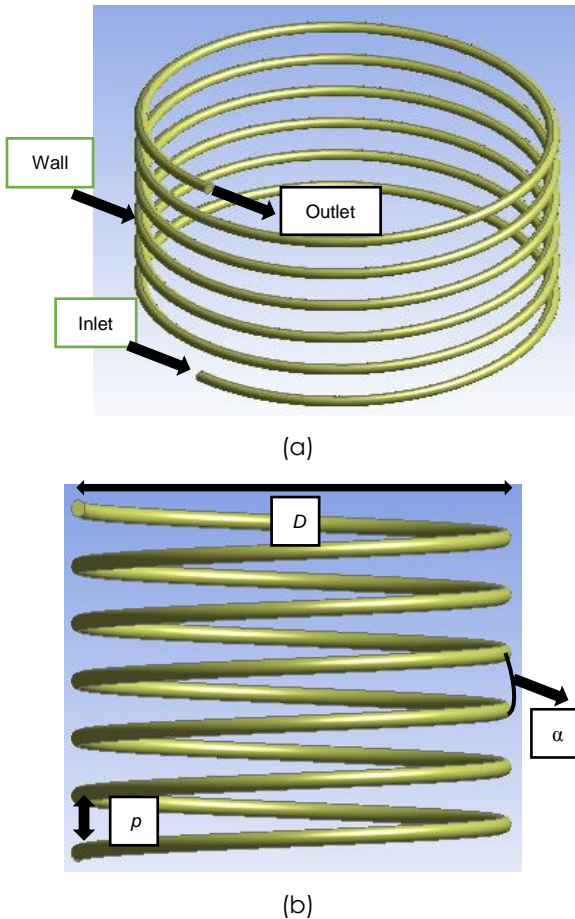

(a)

(b)

Fig. 1. (a) Isometric and (b) front views of helical coiled tube and its boundary conditions.

Table 1. Dimensions of numerical model of helical coiled tube [13]

Coil diam., D (mm)	Inner tube diameter, d (mm)	Length of uncoiled tube, LT (mm)	Pitch, p (mm)	Ascending angle, α (°)	Number of coil turns
283.00	9.00	5500.00	32.00	3.2	6

For the numerical simulation of helical coil tubes, combination of various inlet parameters in terms of pressure, mass flow rate and heat fluxes have been applied to the boundaries of the circular helical coiled tube at constant inlet and outlet temperatures of 27 °C and 120 °C respectively. The applied parameters were referred from the previous researcher's experimental case study. At the inlet of the helical tube, the scCO2 inlet temperature was fixed at 27 °C for all three different inlet pressures. Meanwhile, at the outlet, the temperature is fixed at 120 °C with outlet pressure near to inlet pressure. Uniform heat flux was assigned at the wall of the coiled tube. There were 9 different sets of input parameters, which are labelled as Coil 1 until Coil 9. Table 2 shows the parameters that are obtained from the previous study, applied for the helical coiled tubes at constant inlet and outlet temperatures of 27°C and 120°C. Meanwhile, for each inlet pressure, three different inlet mass flow rates, ṁ (kg/s) are considered. The thermophysical properties are obtained at various inlet pressure for density, ρ (kg/m3), specific heat capacity, CP (J/kg.K), viscosity, μ (Pa.s) and thermal conductivity, k (W/m.K) from National Institute Science and Technology (NIST) chemistry web book [4].

Table 2. The parameters used for helical coiled tube for scCO2.

Coil 1	Coil 2	Coil 3	Coil 4	Coil 5	Coil 6	Coil 7	Coil 8	Coil 9
$P_1 = 8.00$ MPa			$P_2 = 9.03$ MPa			$P_3 = 10.05$ MPa		
$\dot{m}_1$	$\dot{m}_2$	$\dot{m}_3$	$\dot{m}_1$	$\dot{m}_2$	$\dot{m}_3$	$\dot{m}_1$	$\dot{m}_2$	$\dot{m}_3$
0.0131	0.0151	0.0167	0.0131	0.0151	0.0167	0.0131	0.0151	0.0167
$\rho_{avg} = 366.01$ kg/m³			$\rho_{avg} = 405.06$ kg/m³			$\rho_{avg} = 453.27$ kg/m³		

Mesh Independency Test

The designed numerical model of helical coiled tube in SolidWorks is imported into the commercial computational fluid dynamics (CFD) software called ANSYS FLUENT 16.2. Since the mesh quality of any model plays an important role in numerical calculations, mesh independent test was conducted on a circular helical coiled tube for inlet pressure, flow rate and heat flux values of 8.00 MPa, 0.0131kg/s and 20.5 kW/m^2 respectively. This is to check the

mesh sensitivity in terms of various numbers of elements produced in order to choose suitable mesh size for the model. for this, three different mesh sizes (36468 , 53222 and 77140) were simulated at various tube ascending angles. Shown in Fig. 2 is variation of wall temperature at with tube ascending angle at various number of mesh elements. As can be observed from the figure, considering the finest mesh as reference, the maximum percentage differences of the wall temperature T_w for 53222 and 36468 number of mesh elements are only 0.11% and 0.42%, respectively, which are well below the acceptable value. This shows that any of the three mesh sizes can be used for the simulation. In this study, the 77140 numbers of elements is selected for the simulation and the meshed geometry is shown in Figure 2.

Hence, the mesh independency test concludes that the final results from numerical analysis are not affected by the number of mesh elements.
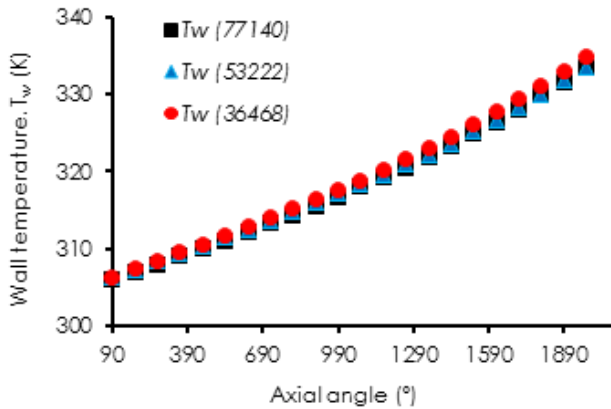

Fig. 2. Mesh independence test comparison for different number of mesh elements.

Validation of the computational Model

To test the reliability of the developed numerical model, the wall temperature results from the current model are compared against the results of other benchmark study. Therefore, the results for helical tube heat exchangers obtained from the present model was validated against the benchmark experimental results by Xu. J. et.al. [13]. Fig. 3 shows variation of wall temperatureu with axial angle. A good agreement can be observed between the results of the present study and the other benchmark result. The maximum percentage errors for Coil-1, Coil-2 and Coil-3 in comparison to the corresponding experimental wall temperature values are 4.9%, 1.7% and 2.6%, respectively. This shows the wall temperatue results obtained by the present model are located within the allowable error ranges.

Therefore, the good agreements between the simulated and published results indicate that the current numerical model is reliable to predict the heat transfer and pressure drop characteristics.

3.0 STATISTICAL ANALYSIS

The statistical design chosen for the development and optimization of thermal-hydraulic performance of scCO$_2$ in helically coiled tubes was a two-level general multilevel factorial design (MFD). Application of this methodology requires the appropriate selection of responses, factors and levels. Nusselt number and friction factor were selected as
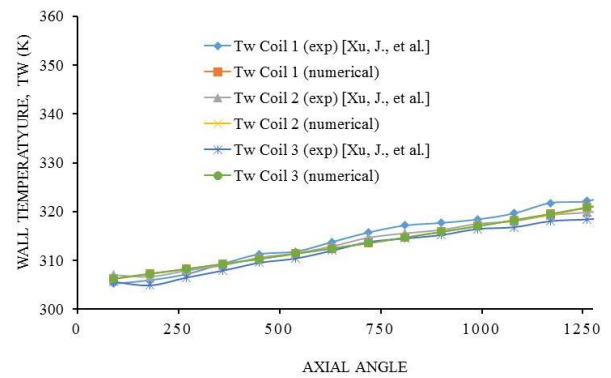

Fig. 3. Variation of wall temperatues with axial angle.

responses. The design determines the effect of each factor on each response as well as how the effect of each factor varies with the change in the level of the other factors, i.e., interactions. If there is interaction between two or more factors, i.e., factors are interdependent, it means that the level of one factor changes the effect of other factors on a specific response. Range and levels of the investigated variables are listed in Table 3. The factors were inlet pressure (X_1), and inlet mass flux (X_2). The upper supercritical inlet pressure level (10 MPa) was chosen for being far enough from the sudo-critical point while the lower limit (8 MPa) as being close to the sudo-critical point of scCO$_2$. The inlet mass fluxes were in the range of 0.0131 to 0.0167 m^3/s.

Once the simulations are performed, the response variables (Nusselt number and friction factor) were fitted as a second-order model in order to correlate the response variables to the independent variables. The general form of the second degree polynomial equation is as follows [7, 14]:

$$Y = a_o + \sum_{i=1}^{n} b_i X_i + \sum_{i=1}^{n} b_{ij} X_i^2 + \sum_{i>j}^{n} \sum_{j}^{n} b_{ij} X_i X_j \quad (7)$$

Where (i =1,2) and (j = 1,2,...9) are the linear and quadratic coefficients, respectively, a is the regression coefficient, n is the number of factors studied and optimized in the experiment.

Table 3. Simulation range and levels of the independent variables

Variables	Codded symbol	Range and levels		
		-1	0	+1
Pressure (MPa)	X1	8	9	10
Mass flow rate (m3/s)	X2	0.0131	0.0151	0.0167

Table 4. Variations of average Nu and f with different inlet pressure and mass flux

Inlet pressure (MPa)	Mass flow rate (m³/s)	Average Nu	Friction factor (f)
8	0.0131	1.9813	0.6256
	0.0151	1.9841	0.4710
	0.0167	1.9558	0.3850
9	0.0131	1.9906	0.5735
	0.0151	1.9900	0.4317
	0.0167	1.9896	0.3538
10	0.0131	2.8242	0.7693
	0.0151	2.8248	0.5790
	0.0167	2.8236	0.4735

4.0 RESULTS AND DISCUSSION

Effects of inlet pressure and mass flux

Variations of average Nu and *f* with different inlet pressure and mass flux are tabulated in Table4. As can be clearly seen from the table, at all pressure values the Nu_{avg} is almost constant as the inlet mass flow flux increases. As expected, the 10 MPa inlet pressure produces the highest average Nu followed by the 9 MPa inlet pressure. The maximum average Nu increment from 8 to 9 MPa and from 8 to 10 MPa inlet pressure are around 1% and 43% respectively. This indicates that at points far from the sudo-critical point of carbon dioxide, the heat transfer is much higher than near the critical region. On the other hand, increasing the heat flux at near critical region will have little effect on the heat transfer performance of $scCO_2$. The different mass fluxes used in each coil did affect the friction factor showing friction factor decrement with increasing mass flux. However, higher friction factor is observed at 8 MPa compared to 9 MPa inlet pressure case. This might be due to the reason that the heat flux was doubled for the 9 MPa case which makes the temperature inside the tube increase, hence higher pressure drop. On the other hand, even though it produces highest heat transfer, the pressure drop for 10 MPa is the highest. Considering the friction factor at 8 MPa as reverence value, the average friction factor decreased by 8% at 9.03 MPa and increased by 22% at 10.05 MPa. The continuous decrement of friction factor coefficients is due to the viscosity of $scCO_2$ itself and the amount of inlet mass flow rate (velocity) applied which affects the frictions along the coil tubes.

Model fitting and statistical analysis

A total of 9 simulations were performed according to a two-factor three-level MFD with none duplicate simulations for fractional points and zero replicates at the center point. Table 5 shows the simulation design matrix for the factorial design and the results of the response variables studied. The first second and third columns of data give -1, 0, and +1 coded factor levels in the dimensionless co-ordinate, and the third and fourth columns give the factor levels on a natural scale (Uncoded values). The simulations were carried out in randomized run order to determine the effect of the factors on two responses: Nusselt number and friction factor.

Table 6 shows the analysis of the main effects and interactions in the form of analysis of variance (ANOVA) for the chosen response together with the test of statistical significance, with a 95% confidence level. The *P*-values are used as a tool to check the significance of the corresponding coefficients. The smaller the *P*-values are, the bigger the significance of the corresponding coefficient [14]. As can be seen in Table 6, the *P*-value of the models (regressions) for Nu and *f*, found by ANOVA, were 0.000 and 0.001, respectively, which indicate that the models are very suitable. On the other hand the interaction terms are not significant. In general, the ANOVA results showed that the generated equations consisting of linear and square (curvature) terms adequately represent the actual relationship between the responses (Nu and *f*) and significant variables (inlet pressure and mass flux). Especially larger F-value with the associated *P*-value (smaller than 0.05, confidence interval) means that the simulation system can be modeled effectively having less error. Therefore, interaction effects as significant model terms can be used for modeling the simulation [15]. In addition, the coefficient determination (R2) values of 100% and

99.4% (for Nu and f respectively), and adjusted coefficient of determination (Adj. R2) of 100% and 98.5% (for Nu and f respectively), indicated that, the accuracy and general availability of the polynomial model were adequate.

After elimination of the insignificant interaction parameters, the final empirical models based on Eq. (7) at 95% confidence level can be represented as follows.

For Nu:

$$Nu = 31.3196 - 6.935 * P - 2.3873\dot{m} + 0.4089P^2 \tag{8}$$

And for f:

$$f = 10.3568 - 1.6869 * P - 275.8581\dot{m} + 0.09687P^2 + 6903.94\dot{m}^2 \tag{9}$$

The comparison of predicted values (using Eqs. 8 and 9) and the actual simulation data are presented in Table 7. It can be seen from the table that the predicted Nusselt number and friction factor are in reasonable agreement with the experimental data. The maximum percentage errors between the actual simulation data and the results obtained using the developed regression equations 8 and 9 for Nu and f are 0.69% and 4.2% respectively. It can be concluded from Table 7 that the ANOVA results were valid since there was no problem with the normality of the simulation data distribution, except with a point corresponding to the middle values of friction factor close to 0.5 where there is error of 4.2%.

Table 5. Simulation design table for the factors and responses

Run	Coded Values		Uncoded Values		Responses	
	P (MPa)	$\dot{m}$ (m3/s)	P (MPa)	$\dot{m}$ (m3/s)	Nu	f
1	0	-1	9	0.0131	1.9906	0.5747
2	-1	-1	8	0.0131	1.9813	0.6256
3	1	1	10	0.0167	2.8236	0.4735
4	-1	1	8	0.0167	1.9558	0.3850
5	0	0	9	0.0151	1.9900	0.4326
6	-1	0	8	0.0151	1.9841	0.4710
7	1	-1	10	0.0131	2.8242	0.7693
8	1	0	10	0.0151	2.8248	0.5790
9	0	1	9	0.0167	1.9896	0.3538

Table 6. ANOVA table for response surface regression

Sources	Degree of freedom	Sequential sum of squares		Adjusted Sum of squares		Adjusted Mean square		F-value		P-value		Remark	
		Nu	f	Nu	f	Nu	f	Nu	f	Nu	f	Nu	f
Regression	5	1.4197	0.13702	1.4197	0.1370	0.2839	0.02740	5176.8	106.2	0.000	0.001	Sig	Sig
Linear	2	1.0851	0.11651	1.0851	0.1165	0.5409	0.05759	9861.3	223.2	0.000	0.001	Sig	Sig
Square	2	0.3345	0.01974	0.3345	0.0197	0.1672	0.00987	3049.1	38.3	0.000	0.007	Sig	Sig
Interaction	2	0.0001	0.00078	0.0001	0.0007	0.0001	0.0007	2.57	3.00	0.207	0.181	InSig	InSig
Residual error	3	0.0002	0.00077	0.0002	0.00077	0.00005	0.00026						
Total	8	1.4198	0.1378										

For Nu : S= 0.00868, R2= 99.97%, Adj R2 = 99.96%, Pred R2 = 99.91%   For f : S = 0.0161, R2= 99.4%, Adj R2 = 98.5%

Sig. = Significant, InSig. = Insignificant

Table 7. Comparison of actual simulation vs predicted data for Nu and f

Nu_simlation	Nu_prediction	Error (%)	f_simlation	f_prediction	Error (%)
1.9558	1.9693	0.69	0.3538	0.3398	3.96
1.9813	1.9779	0.17	0.385	0.3799	1.33
1.9841	1.9732	0.55	0.4326	0.4299	0.63
1.9896	1.9856	0.20	0.471	0.4700	0.21
1.99	1.9895	0.03	0.4735	0.4934	4.21
1.9906	1.9942	0.18	0.5747	0.5922	3.05
2.8236	2.8197	0.14	0.579	0.5835	0.78
2.8242	2.8283	0.15	0.6256	0.6323	1.08
2.8248	2.8236	0.04	0.7693	0.7458	3.05

5.0 CONCLUSION

In the present work, a multilevel factorial design (MFD) with two factors was implemented to study the impacts of inlet pressure and inlet mass flux on the thermal-hydraulic performance of ScCO2 flowing through vertical helically coiled circular tubes. It was observed from the actual simulation results that inlet pressure has no significant effect on the Nusselt number while varying the mass flow rate affected the Nu significantly. On the other hand, increments of both inlet pressure and mass flux have decreased the friction factor. Thus, it can be concluded from the simulation results that high pressure inlet is recommended where high heat transfer is required, whereas low inlet pressure is recommended where pumping power is a crucial issue. The experimental design studies showed that linear and square effects of pressure and mass flow rate are more significant than the interaction term and they have a positive effect on both Nusselt number and friction factor. It is proved that a multilevel-factorial design was an effective study for determining the influence of the inlet pressure and mass flow rate on the thermal-hydraulic performance of ScCO2 heating process.

Acknowledgement

References

[1] W. Zhang, S. Wang, C. Li, and J. Xu, "Mixed convective heat transfer of CO2 at supercritical pressure flowing upward through a vertical helically coiled tube," Applied Thermal Engineering, vol. xxx, pp. 1-10, 2014.

[2] K. D. Hagen, Heat Transfer with Applications: Prentice Hall, 1999.

[3] Z. B. Liu, Y. L. He, Y. F. Yang, and J. Y. Fei, "Experimental study on heat transfer and pressure drop of supercritical CO2 cooled in a large tube," Applied Thermal Engineering, vol. 70, pp. 307-315, 2014.

[4] E. W. Lemmon, M. O. McLinden, and D. G. Friend. (2015). "Thermophysical Properties of Fluid Systems" in NIST Chemistry WebBook, NIST Standard Reference Database Number 69, Eds. P.J. Linstrom and W.G. Mallard. Available: http://webbook.nist.gov

[5] T. H. Kim, J. G. Kwon, S. H. Yoon, H. S. Park, M. H. Kim, and J. E. Cha, "Numerical analysis of air-foil shaped fin performance in printed circuit heat exchanger in a supercritical carbon dioxide power cycle," Nuclear Engineering and Design, vol. 288, pp. 110-118, 2015.

[6] N. T. Rao, A. N. Oumer, and U. K. Jamaludin, "State-of-the-art on flow and heat transfer characteristics of supercritical CO2 in various channels," The Journal of Supercritical Fluids, vol. 116, pp. 132-147, 2016.

[7] S. M. Seyed Shahabadi and A. Reyhani, "Optimization of operating conditions in ultrafiltration process for produced water treatment via the full factorial design methodology," Separation and Purification Technology, vol. 132, pp. 50-61, 8/20/ 2014.

[8] Y. A. Cengel and J. M. Cimbala, Fluid Mechanics: Fundamentals and Applications. New York: McGraw-Hill, 2013.

[9] A. Oumer, N. Hamidi, and I. M. Sahat, "Numerical prediction of flow induced fibers orientation in injection molded polymer composites," in IOP Conference Series: Materials Science and Engineering, 2015, p. 012066.

[10] A. N. Oumer and O. Mamat, "Numerical modelling of non-isothermal flow of fibre suspensions: prediction of fibre orientation in three-dimensional cavities," International Journal of Computational Science and Engineering, vol. 9, pp. 247-256, 2014.

[11] A. N. Oumer and O. Mamat, "A study of fiber orientation in short fiber-reinforced composites with simultaneous mold filling and phase change effects," Composites Part B: Engineering, vol. 43, pp. 1087-1094, 2012.

[12] Y. A. Cengel and A. J. Ghajar, Heat and Mass Transfer: Fundamentals and Applications, 4th Edition ed. New York: McGraw-Hill Higher Education, 2011.

[13] J. Xu, C. Yang, W. Zhang, and D. Sun, "Turbulent convective heat transfer of CO_2 in a helical tube at near-critical pressure," International Journal of Heat and Mass Transfer, vol. 80, pp. 748-758, 2015.

[14] M. Kılıç, B. B. Uzun, E. Pütün, and A. E. Pütün, "Optimization of biodiesel production from castor oil using factorial design," Fuel Processing Technology, vol. 111, pp. 105-110, 7// 2013.

[15] T. Mutuk and B. Mesci, "Analysis of mechanical properties of cement containing boron waste and rice husk ash using full factorial design," Journal of Cleaner Production, vol. 69, pp. 128-132, 4/15/ 2014.